

NPS ARCHIVE  
1949  
HUNTER, G.

Thesis  
H95



EXCITATION FUNCTION AND ANGULAR DISTRIBUTION  
OF THE NEUTRONS FROM THE D-D REACTION

By

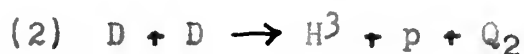
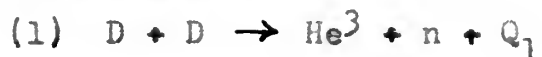
GEORGE TRUMAN HUNTER

A Thesis Submitted in Partial Fulfillment  
of the Requirements for the Degree of  
DOCTOR OF PHILOSOPHY  
at the  
UNIVERSITY OF WISCONSIN

1 9 4 9

## INTRODUCTION

When deuterium is bombarded with deuterons, the following reactions are known to occur:



with  $Q_1 = 3.30 \pm .01 \text{ Mev}^{1,2,3}$  and  $Q_2 = 3.97 \pm .02 \text{ Mev}^4$

The total cross section for each of these reactions has been measured for low energy deuterons and the cross sections have been found to be approximately the same.<sup>5,6,7,8</sup>

---

1 H. V. Argo, Phys. Rev. 74, 1293 (1948).

2 T. W. Bonner, Phys. Rev. 59, 237 (1941).

3 D. L. Livesey and D. H. Wilkinson, Proc. Roy. Soc. A, 195, 123 (Nov. 1948).

4 M. L. E. Oliphant, A. R. Kempton, and Lord Rutherford, Proc. Roy. Soc. 149, 406 (1935).

5 R. B. Roberts, Phys. Rev. 51, 810 (1937).

6 J. H. Manley, J. H. Coon, E. R. Graves, Phys. Rev. 70, 101A (1946).

7 A. C. Graves, E. R. Graves, J. H. Coon, J. H. Manley, Phys. Rev. 70, 101A (1946).

8 E. Bretscher, A. P. French, F. G. P. Seidl, Phys. Rev. 73, 815 (1948).

The angular yields of the neutrons and protons from the reactions have also been measured at low energies and have been found to be similar.<sup>8,9</sup> In the center-of-mass system (CMS) the observed angular distribution was

$$(3) \quad \sigma(\theta) = K (1 + A \cos^2 \theta), \quad \text{where}$$

the coefficients  $K$  and  $A$  are energy dependent and  $\theta$  is the deviation from the deuteron beam direction in CMS coordinates.

Bennett et al.<sup>10</sup> measured the coefficient  $A$  in the angular yield equation for deuteron energies from .5 Mev to 1.8 Mev. Konopinski and Teller<sup>11</sup> have attempted a theoretical explanation of the yield and angular distributions from the D-D reactions. They concluded that spin-orbit coupling plays a large part in the reaction and they indicated a need for more detailed study of the differential cross section. Blair et al.<sup>12</sup> have recently measured the total cross sections and angular yields for both protons and He<sup>3</sup> particles from the D-D reactions for energies from 1 Mev

---

9. A. E. Kempton, B. C. Brown, R. Maasdorp, Proc. Roy. Soc. 157, 386 (1936).

10 W. E. Bennett, C. E. Mandeville, and H. T. Richards, Phys. Rev. 69, 418 (1946).

11 E. J. Konopinski and E. Teller, Phys. Rev. 73, 822 (1948).

12 J. M. Blair, G. Freier, E. Lampi, W. Sleator, Jr., J. H. Williams, Phys. Rev. 74, 1599 (1948).

to 3.5 Mev and have found the cross sections for the two reactions approximately the same. For most deuteron energies they were able to investigate the angular yield of  $\text{He}^3$  only between  $15^\circ$  and  $80^\circ$  in CMS coordinates. In this angular range, they could fit their data with an equation of the form

$$(4) \quad \sigma(\theta) = K (1 + A \cos^2 \theta + B \cos^4 \theta)$$

where K, A, and B are all functions of the bombarding deuteron energy. Curtis, Rosen and Fowler<sup>13</sup> have measured the differential cross section for the production of  $\text{He}^3$  particles from the D-D reaction (1) at 10.2 Mev bombarding energy and have found it to be approximately independent of angle from  $70^\circ$  to  $130^\circ$  measured in CMS coordinates.

For an understanding of the D-D reaction, a McKibben plot<sup>14</sup> of the energy-angle relations for the neutrons will be of value. Such a plot for the neutrons is given in Fig. 1. This plot shows the variation in neutron energy as a function of angle in laboratory coordinates for each bombarding energy. This chart also gives the relation between angles in laboratory and CMS coordinates and allows quick calculation of the ratios of solid angles in the two systems (See caption, Fig. 1) In this paper,  $\phi$  will

---

<sup>13</sup> B. R. Curtis, L. Rosen, J. L. Fowler, Phys. Rev. 73, 648A (1948), also L. Rosen, J. L. Fowler, B. R. Curtis, LADC #425.

<sup>14</sup> J. L. McKibben, Phys. Rev. 70, 101A (1946). Large scale plots for a number of reactions are available from the Atomic Energy Commission, as MDDC-223.

represent angles measured in laboratory coordinates and  $\Theta$  will represent angles measured in CMS coordinates.  $0^\circ$  for both cases is for particles emitted in the same direction as the bombarding deuterons.

As can be seen from Fig. 1, in the backward direction where  $\phi = 180^\circ$ , the neutron energies vary from 1.9 Mev to about 1.6 Mev for bombarding energies between .5 Mev and 4 Mev. In the forward direction where  $\phi = 0^\circ$ , for the same bombarding energies, the neutron energies vary from 3.5 Mev to 7.3 Mev. At all other angles, the neutron energies vary between these two extreme cases. A plot for the protons from the D-D reaction (2) has the same general features with slightly different energy values.

The McKibben plot for the  $\text{He}^3$  particles, given in Fig. 2 shows quite a contrast to the plot for neutrons. From Fig. 2 it may be seen that at most bombarding energies it becomes very difficult to resolve angles near  $90^\circ$  in CMS coordinates from measurements which must be made in laboratory coordinates. In addition the  $\text{He}^3$  particles emitted at large angles of  $\Theta$  would have very short ranges (less than 3 mm in air) and would be difficult to detect.

When the angular yield of the D-D reaction is to be studied by counting the yield of charged particles from the target it is necessary to be able to discriminate between  $\text{He}^3$  particles (which for certain bombarding energies and at some angles may have two different energies),  $\text{H}^3$

particles (which also may have two different energies), disintegration protons and scattered deuterons.

The difficulties of angular resolution and particle discrimination limited the data of Blair et al.<sup>12</sup> to angles less than  $90^\circ$  ( $\theta$ ). In contrast with these difficulties the neutrons from the D-D reaction are monoenergetic in each direction and the yield in all directions except angles close to  $\theta = 180^\circ$  may be measured.

In order to make good measurements of the angular yield of neutrons from the D-D reaction, it is desirable to have a neutron counter which subtends a relatively small solid angle, and one which is relatively insensitive to variations in neutron energies. Such a counter has recently been made available<sup>15</sup> in the form of a shielded long counter for neutrons and it will be discussed later on in this paper.

Because the two particles initiating the D-D reaction are identical, the angular yield of particles in the center-of-mass system must be symmetrical about  $\theta = 90^\circ$  and experimentally this symmetry has been found at low energies.<sup>9,16</sup>

---

<sup>15</sup> A. O. Hanson and J. L. McKibben, Phys. Rev. 72, 673 (1947).

<sup>16</sup> R. O. Maxby, J. S. Allen, and J. H. Williams, Phys. Rev. 55, 140 (1939).



This symmetry condition provides a good check on experimental data. Of course the neutron yield in laboratory coordinates will be quite asymmetric about  $\phi = 90^\circ$  because of the variation in the ratio  $\sin \theta d\theta / \sin \phi d\phi$  as a function of angle. A plot of this ratio as a function of angle in laboratory coordinates for several bombarding energies is given in Fig. 3.

## EXPERIMENTAL ARRANGEMENTS

The Wisconsin electrostatic generator<sup>17</sup> was used as a source of bombarding deuterons for a thin deuterium gas target. Fig. 4 shows the arrangement of the equipment for the experiment. The deuteron beam was magnetically analyzed and brought to the target (T) through a twenty-foot extension of the generator accelerator tube. The high resolution electrostatic analyzer which was available was not used since it was necessary to use targets of 50-150 kev in stopping power to give satisfactory counting rates and minimize background neutrons. However, the generator was automatically controlled to about  $\pm 5$  kev by a corona spray current control circuit.<sup>18</sup> A beam of a few tenths of a microampere and 3 mm diameter was delivered at the target.

---

17 R. G. Herb, C. M. Turner, C. M. Hudson, R. E. Warren, Phys. Rev. 58, 579L (1940).

18 Similar to the circuit reported by J. L. McKibben, and U. H. Frisch, J. M. Hush, Phys. Rev. 70, 117A (1946).

Fig. 5 shows the constructional details of the target and its support. The target chamber (T) consisted of a thin walled brass cylinder 17 mm in diameter, its axis parallel to the deuteron beam. The gas target was separated from the vacuum in the extension tube by a .00005 inch (about one micron) nickel foil.<sup>19</sup> The foil was completely free from pinholes and was sealed with black wax over a 6 mm diameter aperture. Nickel was chosen on the basis of mechanical strength, stopping power, and low neutron yield from bombarding deuterons. Tests on the foil showed that when sealed to the above aperture it could support a maximum pressure differential of 25 p.s.i. The stopping power of the foil varied from 150 kev at a bombarding energy of .71 Mev to 75 kev at a bombarding energy of 3.78 Mev. The average stopping power for protons of energy slightly higher than the  $\text{Li}(p,n)$  threshold was measured from the difference in the generator energies for the thresholds of the  $\text{Li}(p,n)$  reaction measured first as the beam struck the lithium target without passing through the foil and then measured when the beam passed through the foil and struck the lithium. Stopping power of the nickel foil for deuterons was calculated from this measured value. The variation with

---

<sup>19</sup> Available from the Chromium Corporation of America, Waterbury 90, Conn.

energy of the stopping power of nickel was calculated from the variation of the atomic stopping power for copper given in a table in Livingston and Bethe.<sup>20</sup>

The deuteron beam passed through 2 cm. of gas in the target chamber and was then stopped by a .1 mm gold foil. The target chamber could be evacuated and then filled with hydrogen or deuterium through electrically heated palladium tubes and appropriate valves. The pressure of the gas target was calculated from readings on a specially calibrated Bourdon gauge and an accompanying barometer. Pressure readings were accurate to a few per cent.

A small end-window proportional counter (P-Fig. 4) was used to count the disintegration protons from reaction (2) as a monitor of the D-D reaction while the angular distribution of neutrons was being measured at a given bombarding energy. This counter was fixed at  $\theta = 90^\circ$  and 10 cm from the target center. A small hole in the side of the target chamber was covered by a .0025 mm nickel foil which allowed the disintegration protons to reach the counter. The foil and air stopping powers were such that no other particles were counted.

Special precautions had to be taken to keep the neutron background low compared to the neutrons from the thin deuterium gas target. Since light elements bombarded by even low energy deuterons give copious emission of neutrons,

---

<sup>20</sup> M. S. Livingston and H. A. Bethe, Rev. Mod. Phys. 9, 272 (1937).

heavy elements <sup>5</sup> such as gold or tantalum were used wherever possible as the surface that the deuteron beam might strike. A beam-defining tantalum diaphragm allowed the deuteron beam to strike an area 3 mm in diameter only near the center of the target entrance foil. This diaphragm was electrically heated to prevent pump oil in the vacuum system from condensing on the diaphragm where the oil would give off neutrons when struck by the deuteron beam. Shields consisting of water, paraffin, or cement blocks were installed as shown by the shaded areas in Fig. 4 to reduce background counts of neutrons produced by deuterium beams striking in the analyzers. This shielding reduced background by a factor of more than two. A thin sheet of cadmium covered the face of the counter to remove thermal neutrons coming from the room. This had little effect on background of  $0^\circ$  but reduced background by a factor of more than two at  $165^\circ$  ( $\phi$ ). In addition, the target and counter were placed so that a minimum number of neutrons from the reaction would be scattered from the walls of the laboratory into the counter.

The energy-insensitive neutron counter consisted of a proportional counter filled with enriched  $\text{BF}_3$  and embedded in a cylinder of paraffin 20 cm in diameter. A neutron shield, consisting of a layer of boron and about 8 cm of paraffin was an integral part of the counter assembly, surrounding it except for the front face. This shield made

the counter relatively insensitive to scattered neutrons coming from directions other than the front. The distance from target center to counter face was 98 cm. The counter subtended  $\pm 6^\circ$  and a solid angle of .034 steradians. The variation of efficiency with energy of such a counter has been measured by Hanson and McKibben.<sup>15</sup> The efficiency is at its maximum value and is flat ( $\pm 2$  per cent) for neutron energies from .5 Mev to 3 Mev and drops to .95 times the maximum value at 5 Mev (average energy of RaBe neutrons).<sup>21</sup> Extrapolation of this curve would predict an efficiency of .89 times the maximum at 7 Mev. The counter was mounted on a moveable base which was pivoted at a point directly under the target center. Neutrons could be counted at any angle from  $0^\circ$  to  $165^\circ$  in laboratory coordinates.

Beam current entering the insulated target was allowed to charge a polystyrene-dielectric condenser. A string electrometer was used to measure the voltage of the condenser and hence the total charge collected during a run. The charge measurements are good to a few per cent.

---

21 The absolute counter efficiency was one count for an isotropic yield of  $1.34 \times 10^6$  neutrons from a RaBe source 98 cm from the face of the counter.

## PROCEDURE

Background was measured with some hydrogen gas in the target chamber to keep the entrance foil cool. The background neutron yield was measured for the same integrated beam charge as indicated by the string electrometer for positions of the counter at every  $5^\circ$  from  $0^\circ$  to  $165^\circ$  ( $\phi$ ). Counts were then retaken at  $90^\circ$  and  $0^\circ$  to see that conditions had not changed appreciably during the 3 or 4 hour run.

After measuring the background yield at a given energy, the target chamber was evacuated, then filled with deuterium and the angular yield of D-D neutrons measured.

At an average bombarding deuteron energy in the target of .7 Mev, background neutrons amounted to only 2 per cent of the D-D neutron yield. At a deuteron energy of 3.1 Mev, background was about 7 per cent of the total yield in the forward direction but 22 per cent at  $110^\circ$  ( $\phi$ ). At an energy of 3.69 Mev, background was 20 per cent of the total yield at  $0^\circ$  and 68 per cent of the total neutron yield at  $110^\circ$ .

It was found that experimental conditions did not remain constant over the time necessary to take all the data on angular information in this experiment. Therefore special normalizing runs were taken in a short time to

obtain accurate relative values of the total cross sections as a function of energy. Background and total neutron yields were measured only at  $0^\circ$ ,  $90^\circ$ ,  $170^\circ$  in CMS coordinates for each of three or four adjacent bombarding energies at which data had previously been taken. During these measurements only adjustments absolutely necessary to change the bombarding energy were made. These normalizing runs were made at overlapping energies and included all energies from .7 Mev to 3.11 Mev. Due to generator difficulties at the time, it was impossible to normalize the data at .49 Mev, 3.4 Mev, and 3.69 Mev.

The absolute value of the cross section for neutrons from the D-D reaction was determined by using the long counter and the observed angular distribution of neutrons to obtain a comparison of the total neutron flux from the deuterium target with the total neutron flux from a standardized RaBe neutron source.<sup>22</sup> The absolute calibration of the RaBe source is probably not better than  $\pm 5$  per cent.<sup>23</sup>

At a bombarding energy of .7 Mev, the neutron angular yield was measured with two different angular resolutions.

---

22 Calibrated at the Argonne National Laboratories.

23 A similar calibration of the same RaBe source two years earlier (and a few months after the source was pressed) gave a value 20 per cent lower; it is believed that most of this difference resulted from a better mixing (perhaps by diffusion) of the radium and beryllium.



In the first case the front face of the counter subtended an angle of  $\pm 6^\circ$  while in the second the front face of the counter subtended an angle of  $\pm 3^\circ$ . For the latter run the net neutron count was  $1/2.6^{24}$  times the former value while the background count was  $2/3$  times the former value. However, the angular yields in CMS coordinates remained the same within the experimental error. At higher energies, the low neutron yield at  $90^\circ(\theta)$  compared with the background yield made it difficult to make reliable measurements with the higher angular resolution.

---

<sup>24</sup> This does not necessarily imply a departure from the inverse square law since the effective center of the counter is somewhere behind the front face.

## RESULTS

The results to be discussed are for average energies of the bombarding deuterons in the gas target. The lowest average energy was .49 Mev and the highest was 3.7 Mev. These energies were obtained by subtracting the stopping power of the target entrance foil and half the stopping power of the gas target from the generator energy. Because of non-uniformities in the nickel foil and because of uncertainty in the range-energy relation for the foil, the average bombarding energy is probably not known better than  $\pm 10$  kev. The stopping power of deuterium was taken from tables in Livingston and Bethe.<sup>25</sup>

The angular distributions of the neutron yields from the D-D reaction (1) at different energies are plotted as a function of angle in CMS coordinates in Fig. 6. The experimental yields as measured in laboratory coordinates were corrected by the solid angle ratio and by the neutron counter efficiency (for most of the data this correction was much less than 5 per cent and it was never larger than 11 per cent) and then plotted for the corresponding angles in CMS coordinates. The experimental points are plotted

---

<sup>25</sup> M. S. Livingston and H. A. Bethe, Rev. Mod. Phys. 9, 268 (1937).

as circles with RMS statistical deviations indicated at some representative values. The experimentally observed symmetry of the data about  $\theta = 90^\circ$  probably indicates the absence of large unknown systematic errors. The curves plotted in this figure are analytic expressions for the angular yields of neutrons which give good agreement with the experimental points and which were obtained as described in the following paragraphs.

The analytic expressions for the neutron yields are of the form:

$$(5) \quad \sigma(\theta) = K(1 + A\cos^2\theta + B\cos^4\theta + C\cos^6\theta).$$

The coefficients A, B, C, were obtained by making use of the orthogonality properties of Legendre polynomials. Each yield plot is assumed to be of the form:

$$(6) \quad \sigma(\theta) = \sum_{n=0}^m a_n P_n(\cos\theta)$$

where  $P_n$  is the Legendre polynomial of the first kind and  $a_n$  is a real coefficient.<sup>26</sup> By making the integration of the following form:

$$(7) \quad \int_{-1}^{+1} Y(\cos\theta) P_n(\cos\theta) d(\cos\theta) = a_n \left( \frac{2}{2n+1} \right)$$

---

<sup>26</sup> R. Taschek and A. Hemmendinger, Phys. Rev. 74, 373 (1948).

the coefficients  $a_n$  were found. By simple substitution in Eq. 6 the yield formula was converted to the more familiar form of Eq. 5.

When the integrations were carried out on a point-to-point basis, in some cases the experimental errors of the points did not allow the coefficients to vanish for  $n = 3$  or 4. Therefore, the series of polynomials was terminated as soon as the coefficient  $a_n$  reached a value which might be produced by the uncertainty of the experimental data. Also it was considered reasonable that the simplest equation which gave a good fit to the experimental points was better than a more complicated one, and that there should be a smooth variation of coefficients as a function of energy. Therefore the coefficients obtained from the above analysis ~~was~~ modified in some cases. The data at all energies requires finite values for the coefficients A and B and above 2 Mev better fit of the data is obtained if a finite value of the coefficient C is included. Where only A and B are used, the uncertainty in their individual values is about  $\pm 3/10$  of a unit. When all three coefficients are used, there is considerably more leeway in choosing the values of the individual coefficients for a good fit of the data. This is quite evident from the curves given in Fig. 7.

Fig. 7 shows the experimental data for an average bombarding energy of 3.11 Mev and three different analytic expressions for the yield. The dotted curve shows the best

fit of the data possible if no terms higher than  $B\cos^4\theta$  are included. The coefficients for the dashed curve were obtained by the Legendre polynomial analysis which included terms through  $C\cos^6\theta$ . The solid curve has coefficients modified from the analysis results to be consistent with the values at adjacent energies and still give good fit to the experimental data. The data at lower energies required appreciably less modification of the coefficients obtained by the mathematical analysis than was required at this energy.

The coefficients which were finally obtained for the equations for the neutron angular yields are plotted in Fig. 8 and Fig. 9 as a function of energy. Fig. 8 is a plot of the coefficients of the normalized Legendre polynomial components of the neutron wave intensity.<sup>27</sup> Fig. 9 is a plot of the coefficients of the different powers of  $\cos^n\theta$  components of the neutron wave intensity. The extrapolated starting points for the B and C coefficients are approximately indicated by the dotted portions of the two curves. The dotted portion of the curve for the coefficient A is based upon low energy measurements.<sup>8,28</sup> The value of D as the coefficient of a  $\cos^8\theta$ - term was introduced at

---

<sup>27</sup> The symmetry about  $\theta = 90^\circ$  requires that  $a_n = 0$  when n is odd.

<sup>28</sup> R. D. Huntoon, A. Ellett, D. S. Bayley, J. Van Allen, Phys. Rev. 58, 97 (1940).

3.69 Mev rather than have the values of the other coefficients out of line with their values obtained by extrapolation from lower energies. This does not necessarily mean the sudden appearance of a large amount of  $\cos^8\theta$  in the angular yield; it is probably due to the uncertainty in the measurements at this energy. The data taken at 3.69 Mev ~~is~~ quite obviously not in line with data at other energies. ~~It is~~ not considered reliable because background was large and fluctuating for this run. For example, a ten per cent fluctuation in background could make a 20 per cent change in the net neutron yield for angles near  $\theta=90^\circ$ .

The ratios of the neutron yields at  $0^\circ$  to the neutron yields at  $90^\circ$  in the center-of-mass system is:

$$(8) \quad \frac{N(0^\circ)}{N(90^\circ)} = 1 + A + B + C + D$$

These ratios have been plotted as a function of energy in Fig. 10. These ratios are known much more accurately than are the individual coefficients because of the latitude in the choice of the coefficients for a good fit of the experimental points. These ratios allow the comparison of the results of this experiment with other experimental results which may <sup>not</sup> have as complete angular information. For purposes of comparison the results of Blair et al.,<sup>12</sup> Bennett et al.,<sup>10</sup> and the proton results of Huntoon et al.<sup>28</sup> have also been plotted. In the work done by Blair et al., the coefficients were determined by fitting the experimental points only be-

tween  $10^\circ$  or  $15^\circ$  and  $80^\circ$  in CMS coordinates, without the decided advantage of having the relative yields at  $0^\circ$  and  $90^\circ$ . As is evident from Fig. 10, all four of these experiments show consistent results.

The values of  $K$  in Fig. 9 are based on the absolute value of the efficiency of the neutron counter and the data taken during the normalization runs. The values at .49 Mev, 3.4 Mev, and 3.69 Mev indicated by solid circles are extrapolated from the other values since normalization runs were not taken at those energies. Calculations from unnormalized data indicate that these extrapolated values are probably good within  $\pm 10$  per cent. The experimental values agree quite well with similar values measured by Blair et al.

The differential cross sections for the neutron yields from the D-D reaction are of the form

$$(9) \quad \sigma(\theta) = K (1 + A\cos^2\theta + B\cos^4\theta + C\cos^6\theta)$$

and are plotted as a function of angle in CMS coordinates in Fig. 11. Until the high neutron background at energies above 3.4 Mev can be reduced, 3.4 Mev represents an approximate upper limit at which our data can be considered reliable.

The spherically symmetric yield of  $\text{He}^3$  particles from the D-D reaction at 10 Mev reported by Curtis et al. may not be in violent disagreement with the data at lower energies shown in Fig. 11, for they were able to measure only between angles of  $70^\circ$  and  $130^\circ$  in CMS coordinates and the present data would indicate a trend toward isotropy in this region.

The differential cross section which they report is about  $3.3 \times 10^{-27} \text{ cm}^2$ . This would indicate that the value of  $K$  in Fig. 9 decreases from the value of  $6 \times 10^{-27} \text{ cm}^2$  at 3 Mev to  $3.3 \times 10^{-27} \text{ cm}^2$  at 10 Mev.

When the differential cross sections are plotted in laboratory coordinates they of course become very asymmetric as is seen in Fig. 12.

The total cross section for the neutron yield from the D-D reaction is plotted in Fig. 13 as a function of energy. These values were obtained by integrating the differential cross section. The values indicated at .49 Mev, 3.4 Mev, and 3.69 Mev by solid circles are based on the assumed values of  $K$  as discussed previously. Because of the difficulties in measuring the absolute values of neutron flux, the values of  $\sigma(D,n)$  are probably not better than  $\pm 10$  per cent. However, the relative values are probably much better. For comparison purposes, the values obtained from other experiments<sup>5,7,8,12</sup> have also been plotted. There is remarkably good agreement with the results of Blair, et al.<sup>12</sup> over the entire range of energies and the low energy data<sup>6,7,8</sup> appear to lie in line with the extension of the curve for this experiment. Recent information indicates that  $\sigma(D,n)$  decreases to the value .07 barns at 10 Mev.<sup>29</sup>

---

<sup>29</sup> Verbal communication with R. Taschek concerning the continuing work of Rosen and Fowler at Los Alamos. (See also footnote 13).



The probability  $P_\ell^{30}$  for a pair of deuterons possessing the relative orbital angular momentum  $[\ell(\ell+1)]^{\frac{1}{2}} \hbar$  to penetrate the combined coulomb and centrifugal barriers (maximum radius of interaction assumed to be  $7 \times 10^{-13} \text{ cm}$ )<sup>11</sup> is plotted as a function of the bombarding energy for  $\ell = 0, 1, 2, 3$  in Fig. 9. A more significant quantity is the cross section for penetration to the nuclear surface which is given by

$$(10) \quad \sigma_\ell = \pi \lambda^2 (2\ell + 1) P_\ell$$

These cross sections are plotted in Fig. 14. It is interesting to note that when  $\sigma_\ell (\ell = 1) = \frac{1}{2}$  barn, the coefficient B (Fig. 9) begins to have an appreciable value, and that when  $\sigma_\ell (\ell = 2) = \frac{1}{2}$  barn, the coefficient C begins to have an appreciable value. By analogy with these two cases it would seem reasonable that a coefficient D would begin to have a finite value at a bombarding energy of 3 Mev or above and the experimental data does not exclude this.

The finite value of the coefficient B corresponds to an outgoing D-wave being present in the neutron yield. However, the cross section for an incoming D-wave is very small and the cross section for an incoming P-wave is just becoming appreciable. This would indicate that probably spin-orbit coupling produces the required orbital angular momentum which is found in the outgoing wave and is not

---

30 H. A. Bethe, Rev. Mod. Phys. 9, 178 (1937).

present in the incoming wave.

At a given bombarding energy, the amplitude of the neutron wave is

$$(11) \quad \psi(\theta) = \sum_{n=0}^m a_n e^{iB_n} P_n(\cos\theta),$$

where  $a_n$  is a real amplitude factor,  $e^{iB_n}$  is a phase factor, and  $P_n(\cos\theta)$  is the Legendre polynomial of the first kind. Then the intensity of the neutron wave is

$$(12) \quad I(\theta) = \psi(\theta) \psi^*(\theta).$$

At very low bombarding energies at which the neutron yield intensity may be represented in the form

$$(13) \quad \sigma(\theta) = K (1 + A \cos^2\theta),$$

only s- and p-waves are present and their individual amplitudes may be found. When the intensity includes  $B \cos^4\theta$  or higher terms, a unique determination of the individual amplitudes ( $a_n$ ) and phases ( $B_n$ ) is impossible.

## ACKNOWLEDGEMENT

The writer wishes to express his appreciation to Professor H. T. Richards for his suggestion of the problem and his continued criticism and encouragement; to the members of the Physics Department staff, the graduate students, and technicians who gave valuable assistance; and to the Wisconsin Alumni Research Foundation and the Atomic Energy Commission for their financial support.

FIGURE 1

Energy-angle nomograph for the neutrons from the  $D(D,n)He^3$  reaction. Read  $E_N$  at any angle  $\phi$  as the intersection of the solid circle (of radius C) with the dotted circle (of radius B) determined by  $E_D$ . All energies in Mev. Broken lines intersect dotted circles at equal angles in CMS coordinates.

$$\theta - \phi = \sin^{-1} \left( \frac{A}{B} \sin \phi \right)$$

$$\frac{\sin \theta d\theta}{\sin \phi d\phi} = \frac{E_N}{.3747 (E_D + 6.62) \cos(\theta - \phi)}$$

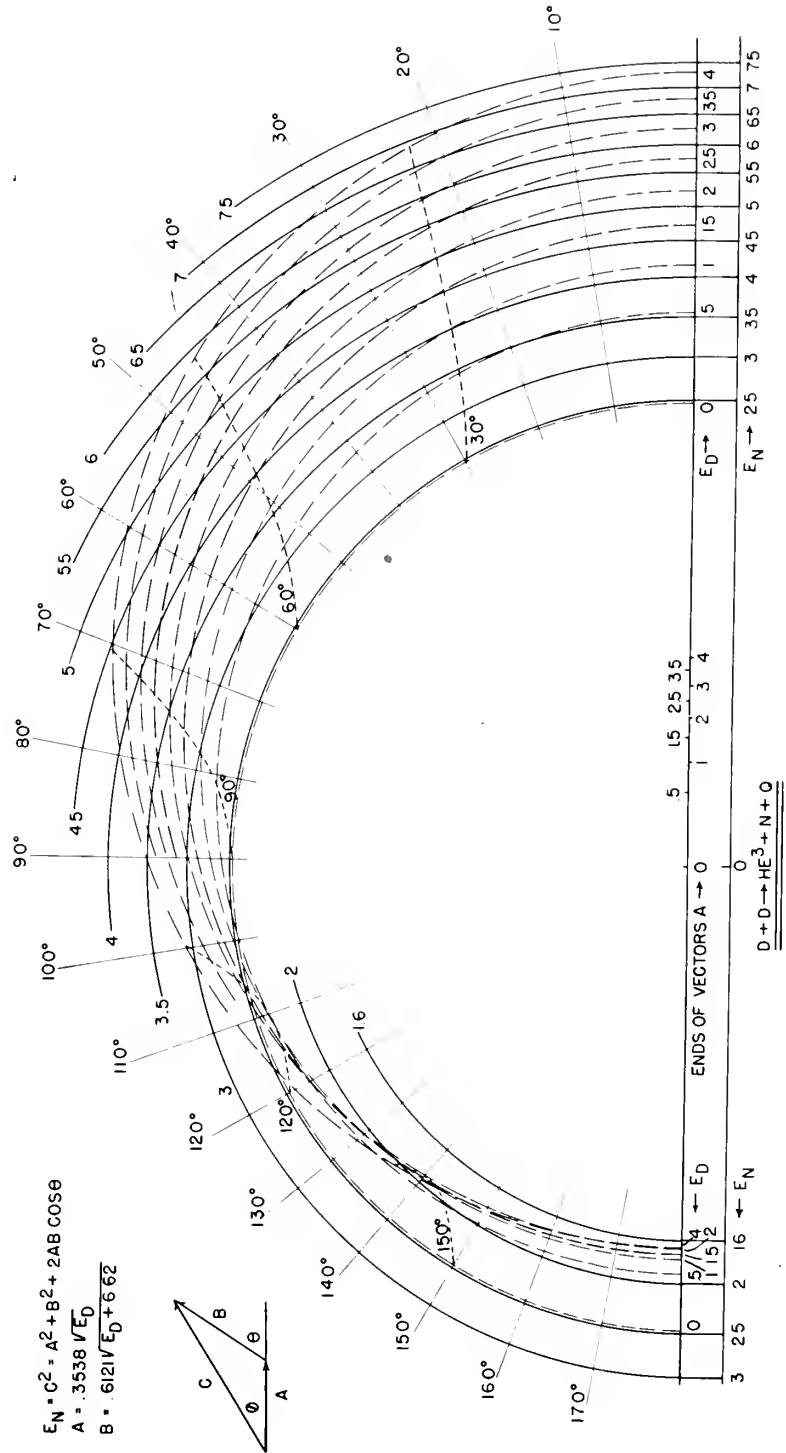


FIGURE 2

Energy-angle nomograph for the  $\text{He}^3$  from the  $\text{D}(\text{D},\text{n})\text{He}^3$  reaction. Read  $E_\alpha$  at any angle  $\phi$  as the intersection of the solid circle (of radius C) with the dotted circle (of radius B) determined by  $E_D$ . All energies in Mev. Broken lines intersect dotted circles at equal angles in CMS coordinates.

$$\theta - \phi = \sin^{-1} \left( \frac{A \sin \phi}{B} \right)$$

$$\frac{\sin \theta d\theta}{\sin \phi d\phi} = \frac{E_\alpha}{.1252 (E_D + 6.62) \cos(\theta - \phi)}$$

( $E_\alpha$  is the energy of the emitted  $\text{He}^3$  particle)

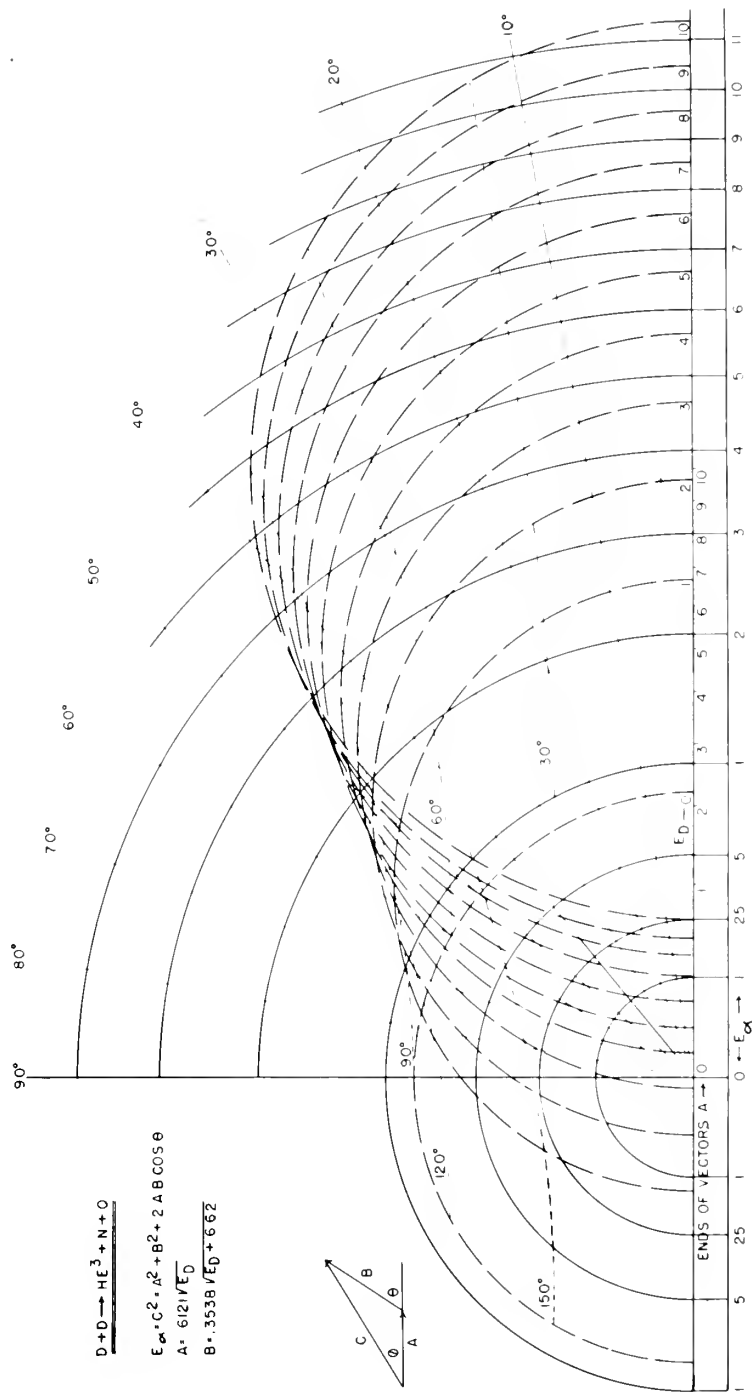


FIGURE 3

Ratio of solid angle in CMS coordinates to solid angle in laboratory coordinates as a function of angle in laboratory coordinates for several bombarding deuteron energies.



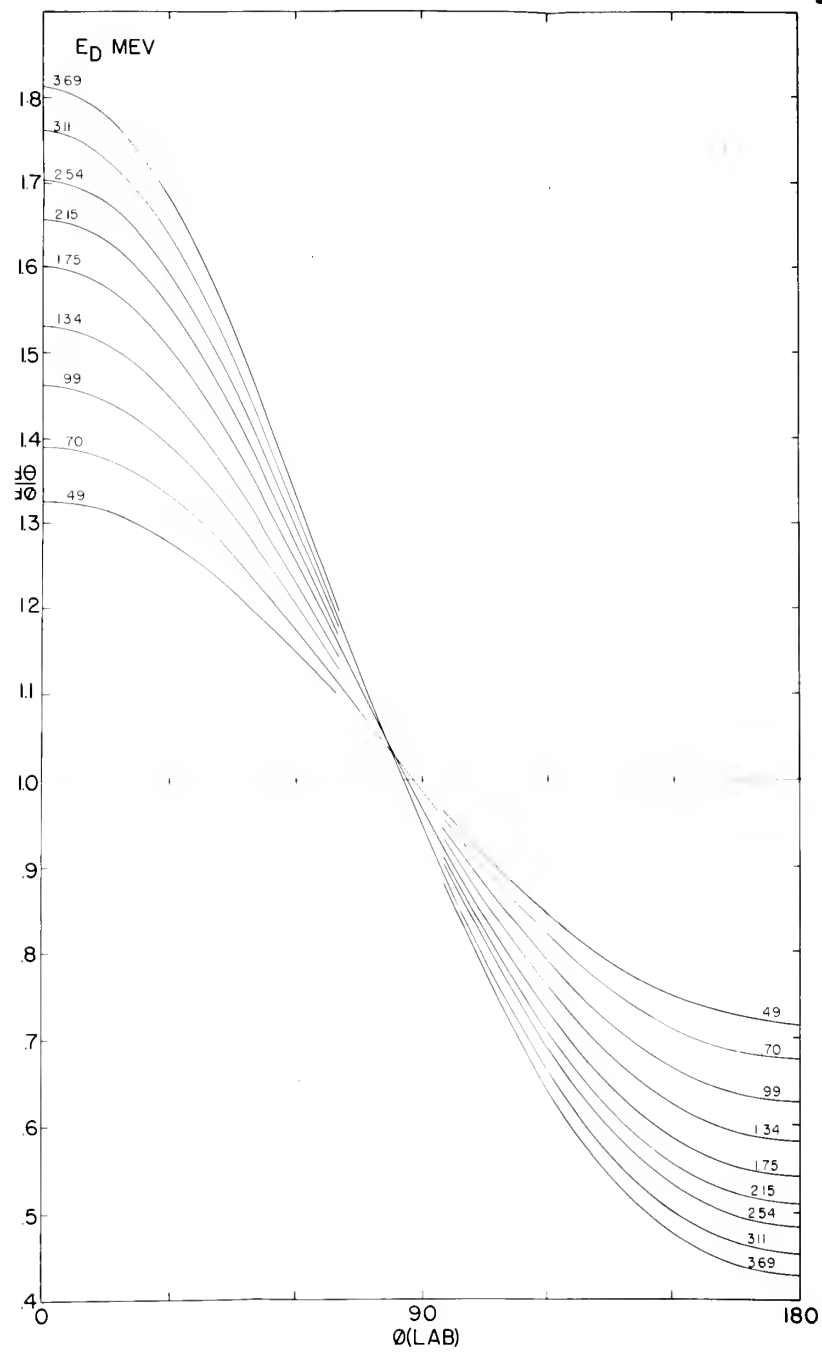


FIGURE 4

Experimental arrangement for measuring  
neutrons from the D-D reaction.

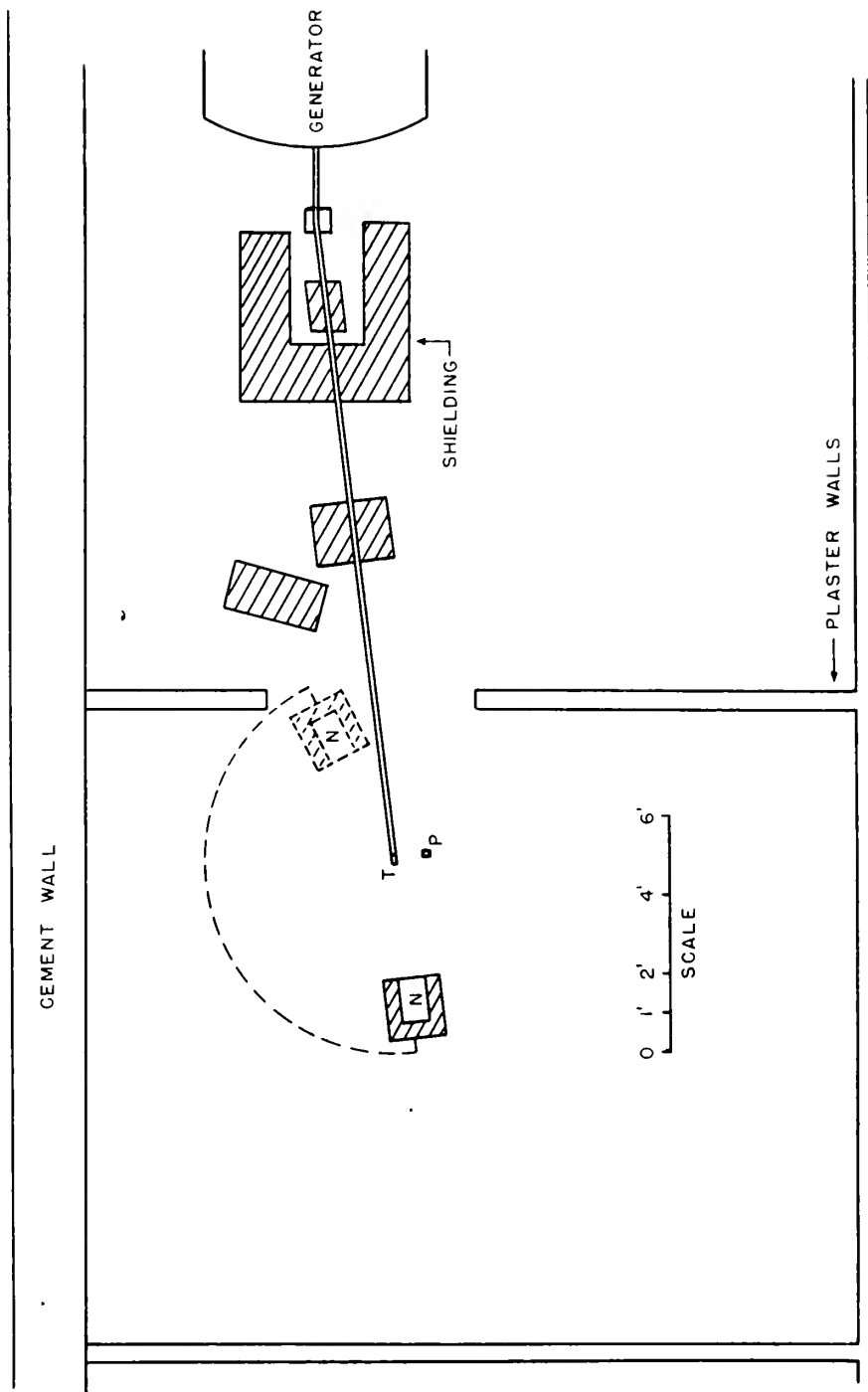


FIGURE 5

Constructional details of gas target  
chamber and support.

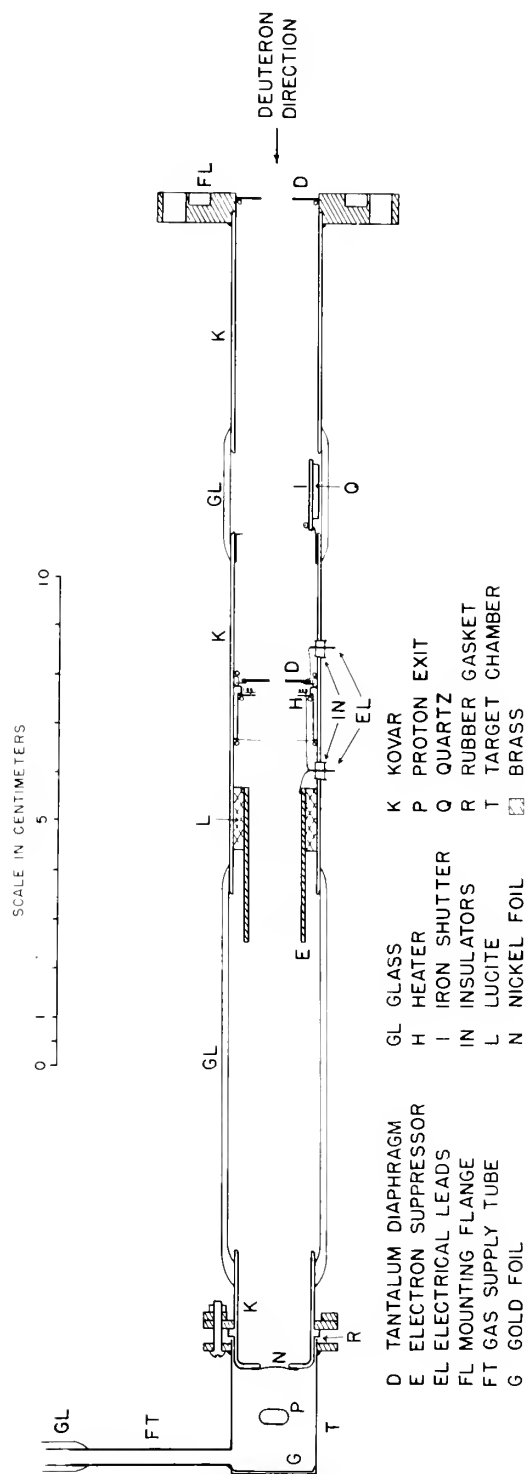


FIGURE 6

Angular distribution of the neutron yield from the D-D reaction as a function of angle in CMS coordinates for several energies. Ordinates shifted to eliminate overlapping.

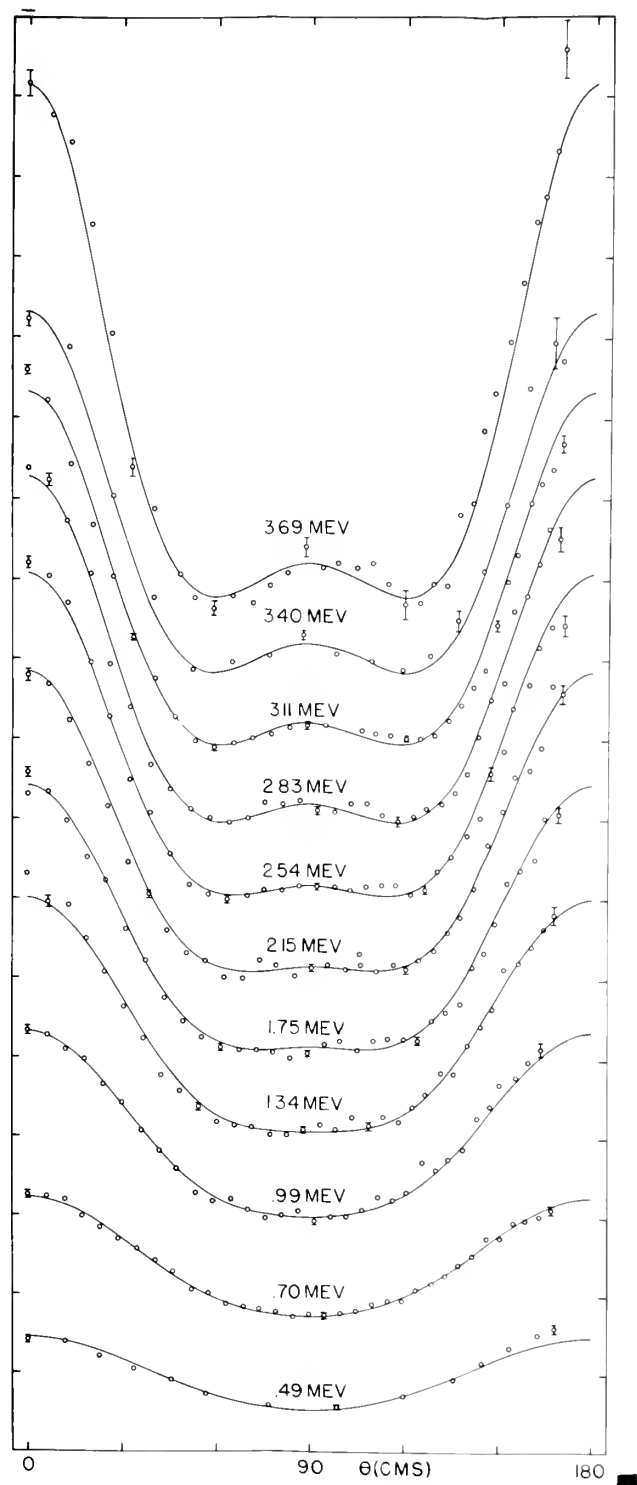


FIGURE 7

Angular yield of neutrons from the D-D reaction of 3.11 Mev as a function of angle in CMS coordinates. Dotted curve is best fit using terms including  $B\cos^4\theta$ . Dashed curve is from polynomial analysis. Solid curve is from analysis coefficients modified to agree with data at other energies and still give good fit to experimental points.



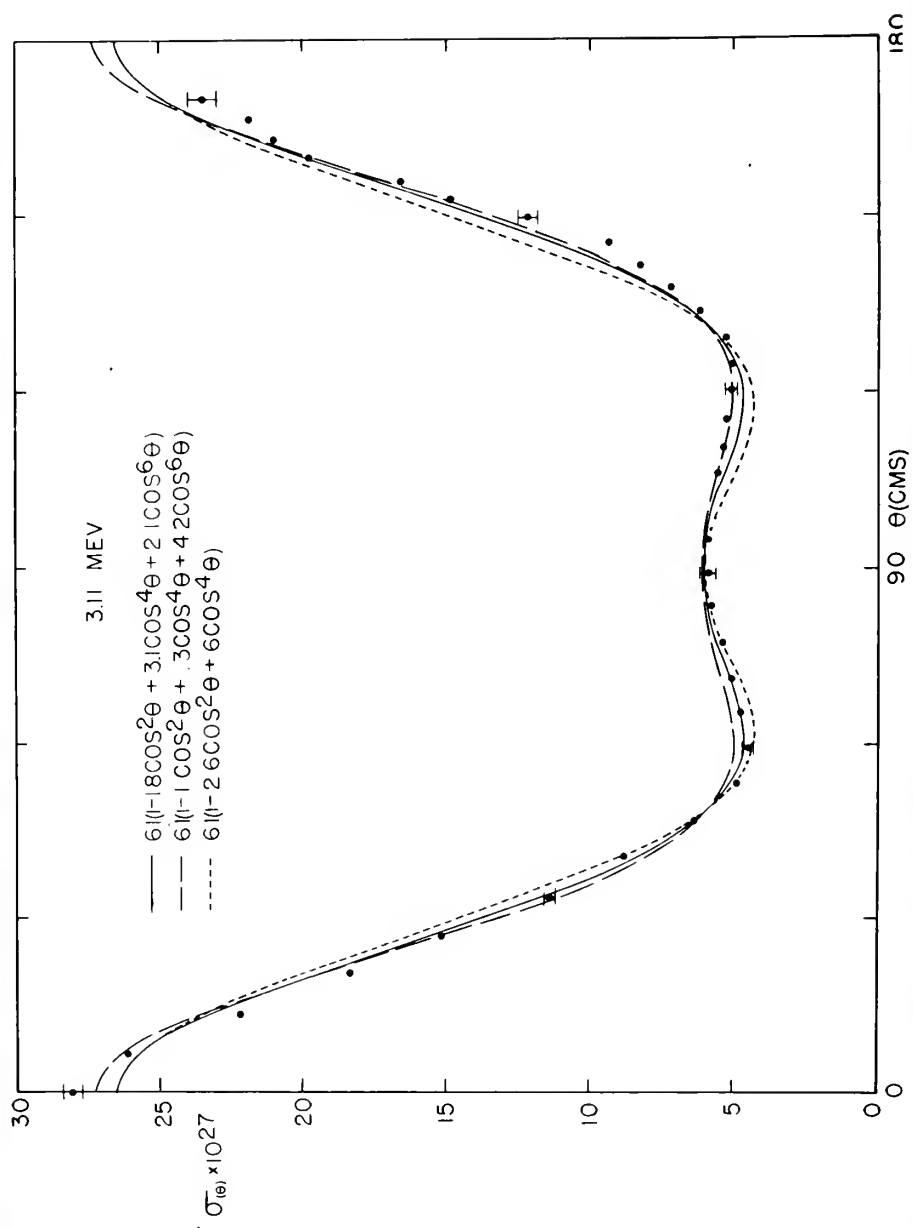


FIGURE 8

Coefficients of normalized Legendre polynomial components of neutron differential cross section from the D-D reaction as a function of bombarding deuteron energy.

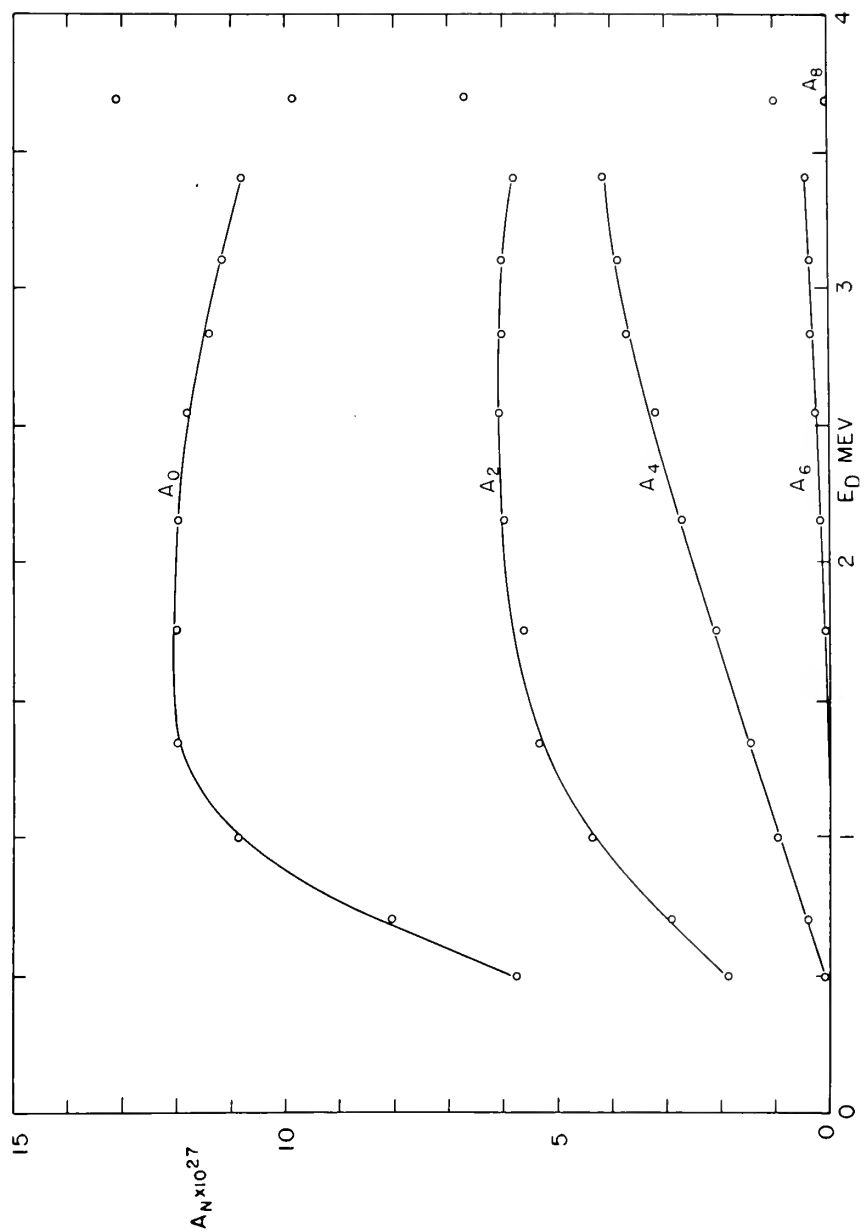


FIGURE 9

Coefficients of  $\cos^n \theta$  components of neutron differential cross section from the D-D reaction as a function of energy. Solid circles obtained by extrapolation. Probabilities of nuclear barrier penetration for two deuterons as a function of bombarding deuteron energy for  $\ell = 0, 1, 2, 3$ .

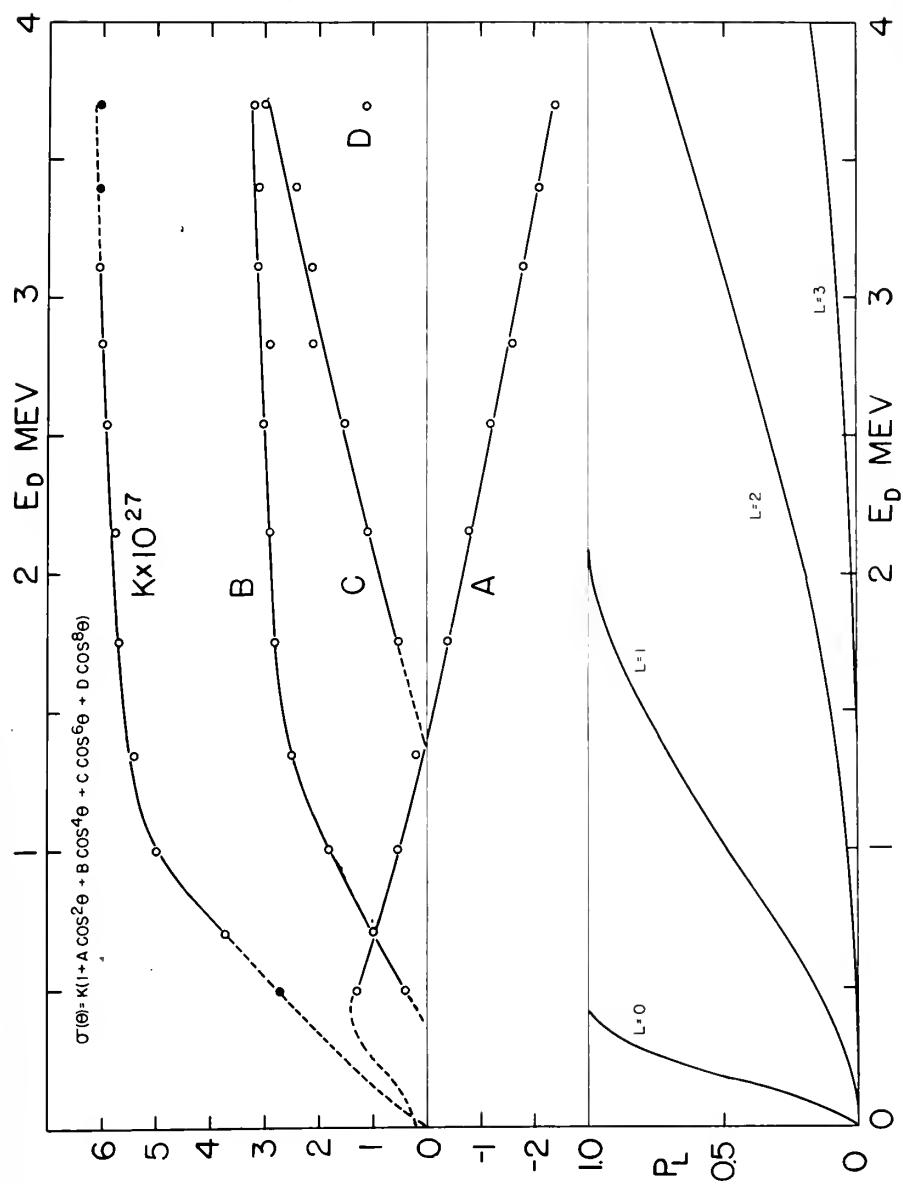


FIGURE 10

ratios of neutron yield at  $0^\circ$  to neutron  
yield at  $90^\circ$  in CMS coordinates as a  
function of bombarding deuteron energy.

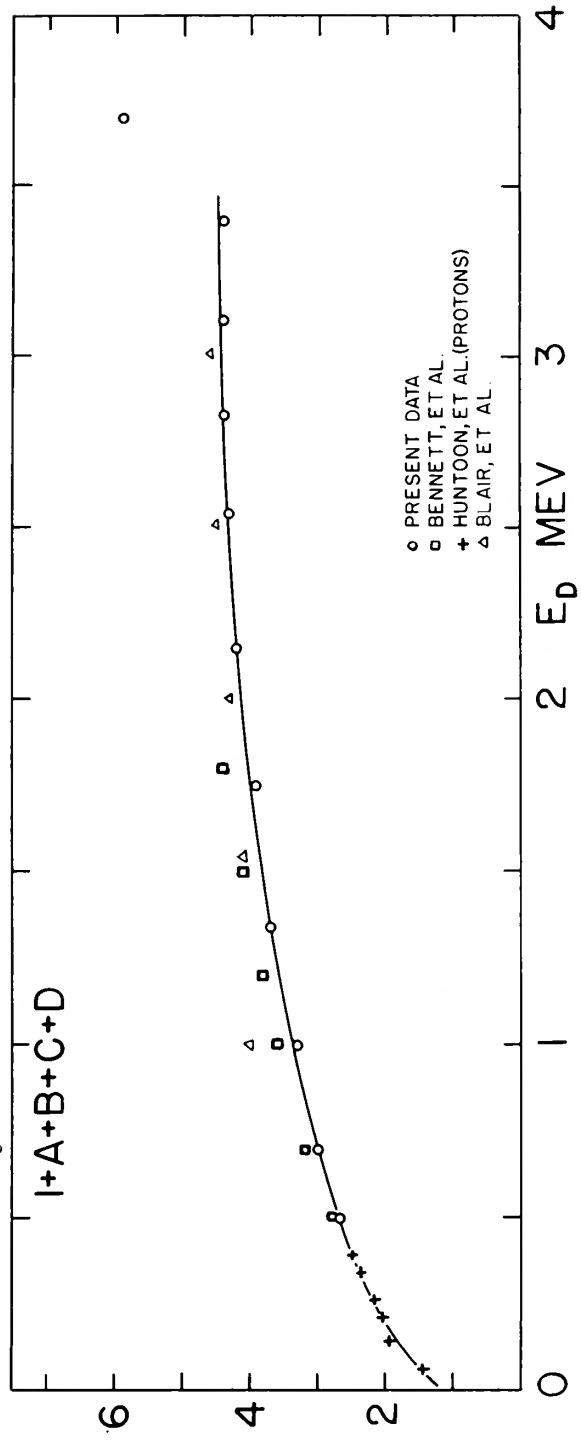


FIGURE 11

Differential cross section for neutrons from the D-D reaction as a function of angle in CMS coordinates for different bombarding deuteron energies.



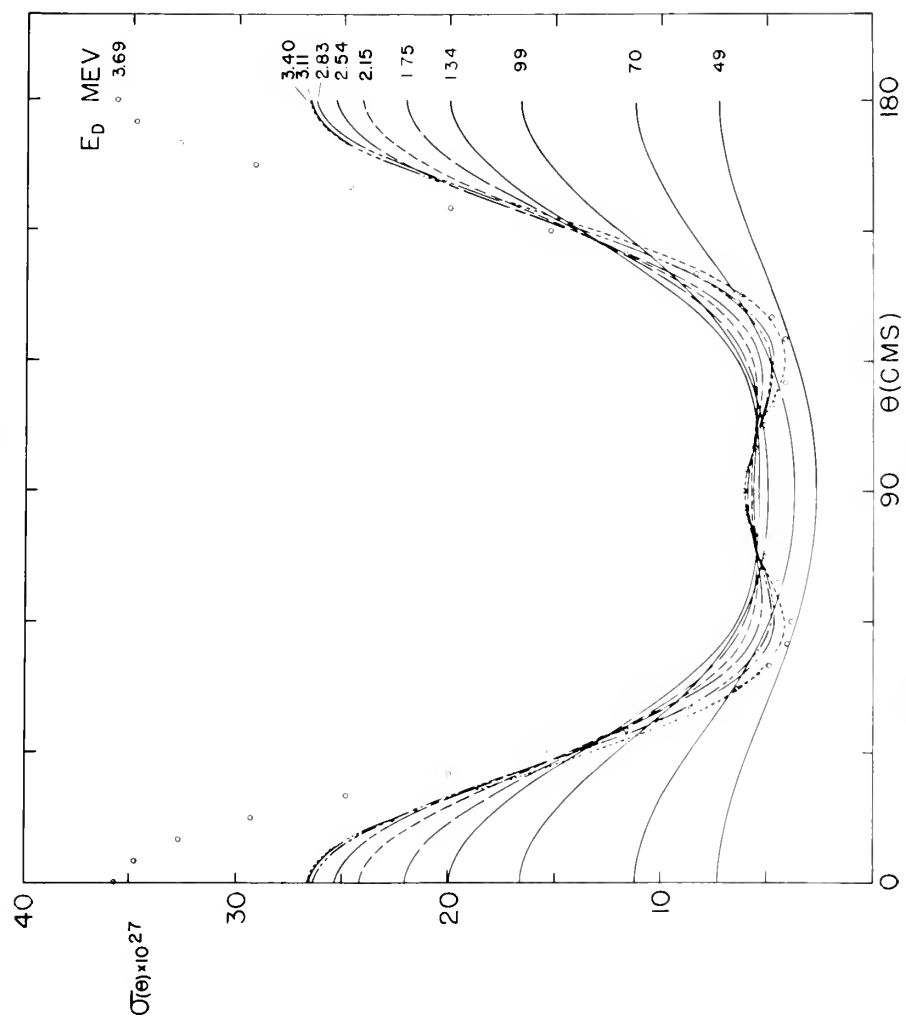


FIGURE 12

Differential cross section for neutrons from the D-D reaction as a function of angle in laboratory coordinates for different bombarding deuteron energies.

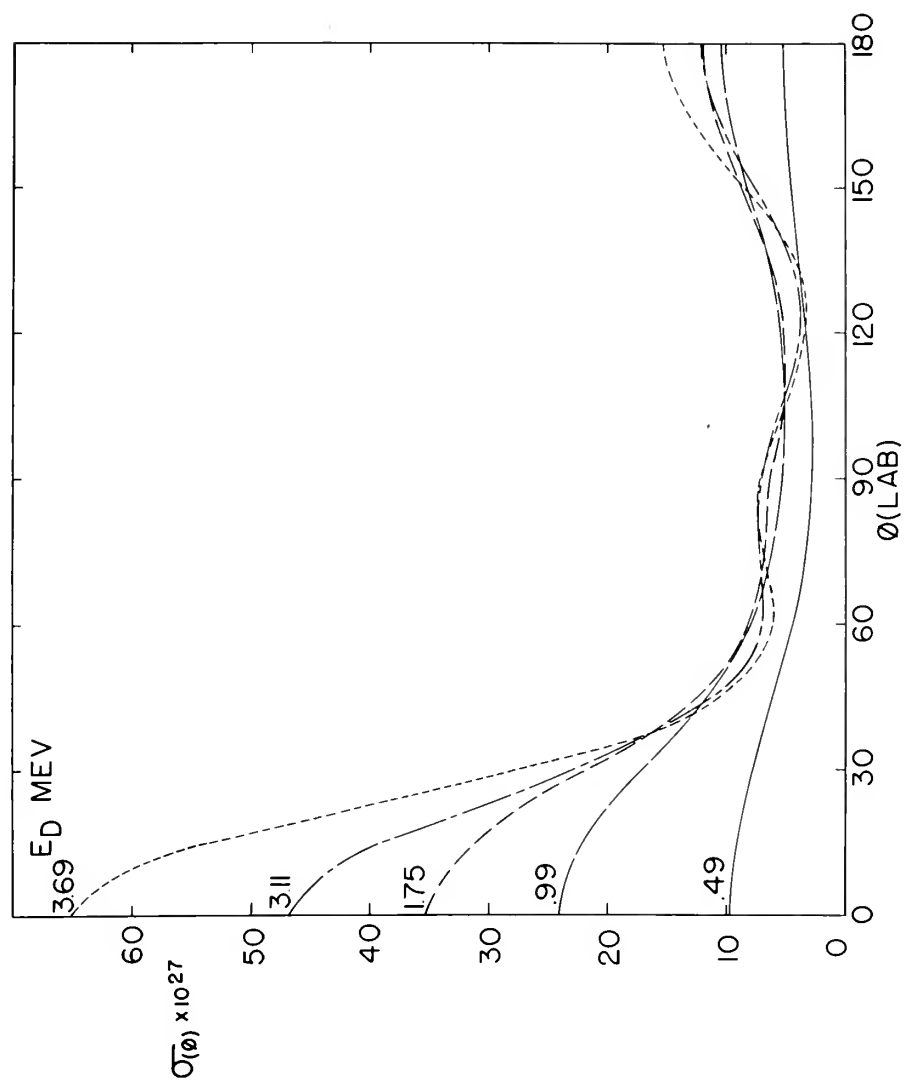


FIGURE 13

Total cross section for the neutrons  
from the D-D reaction as a function of  
bombarding deuteron energy.

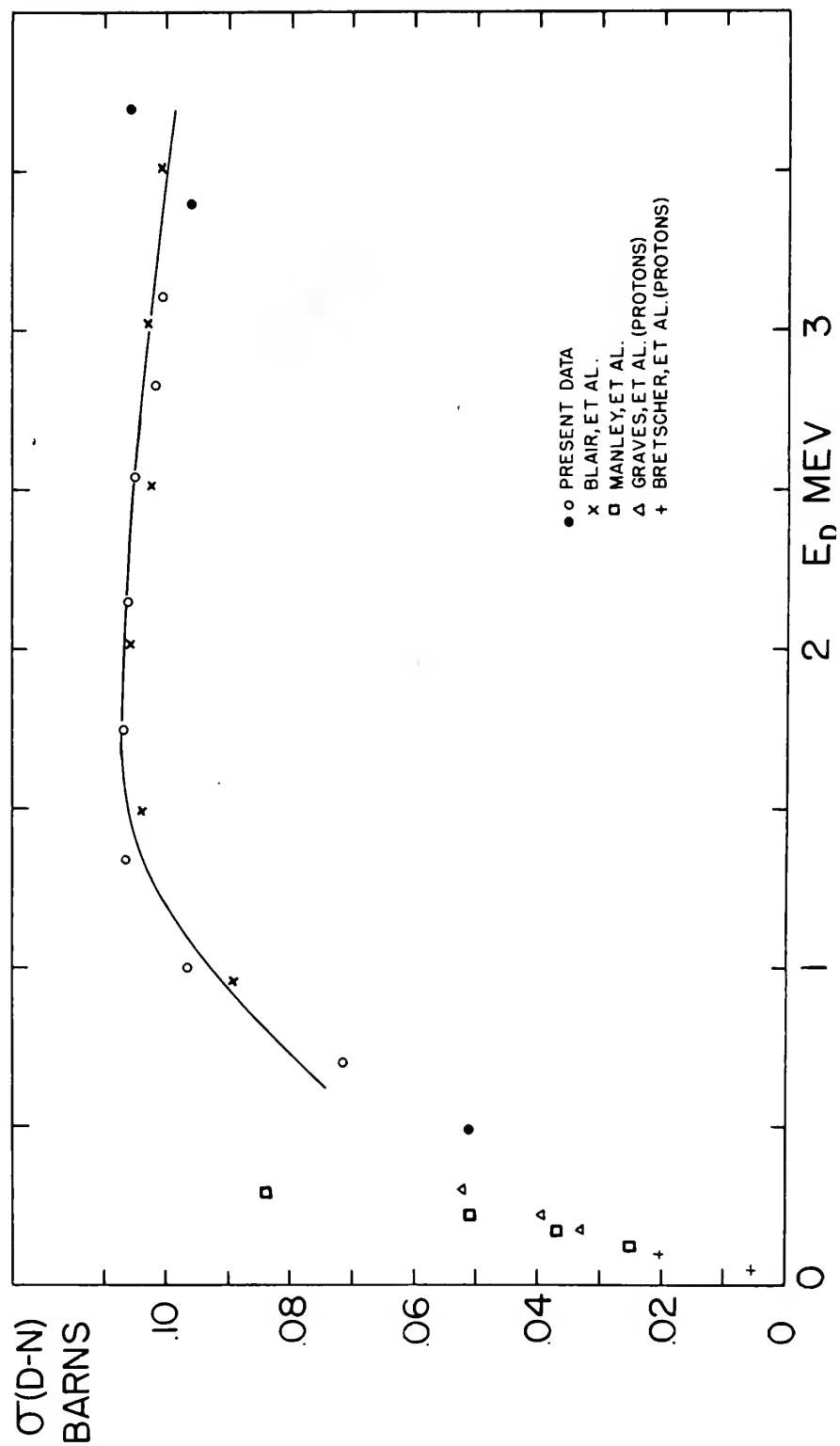
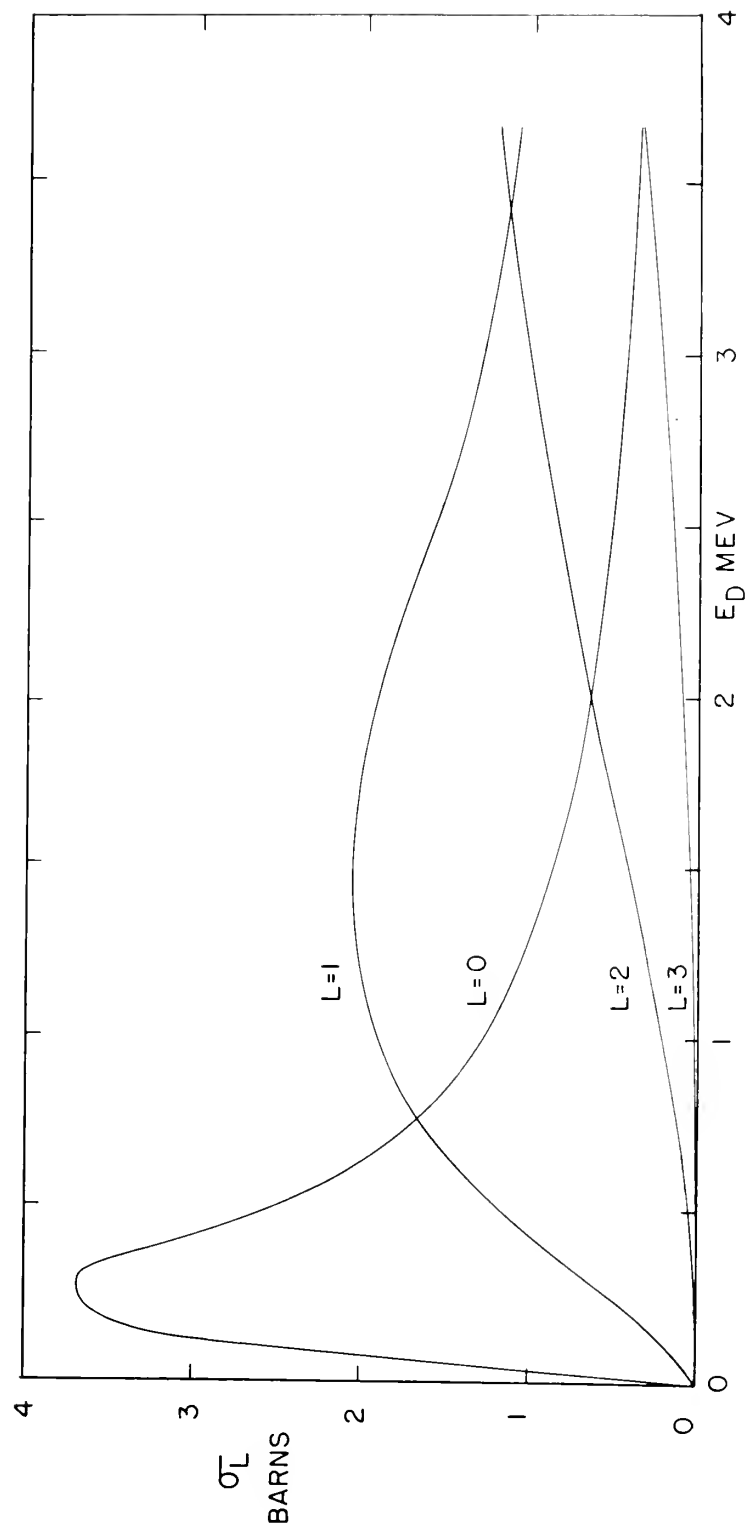


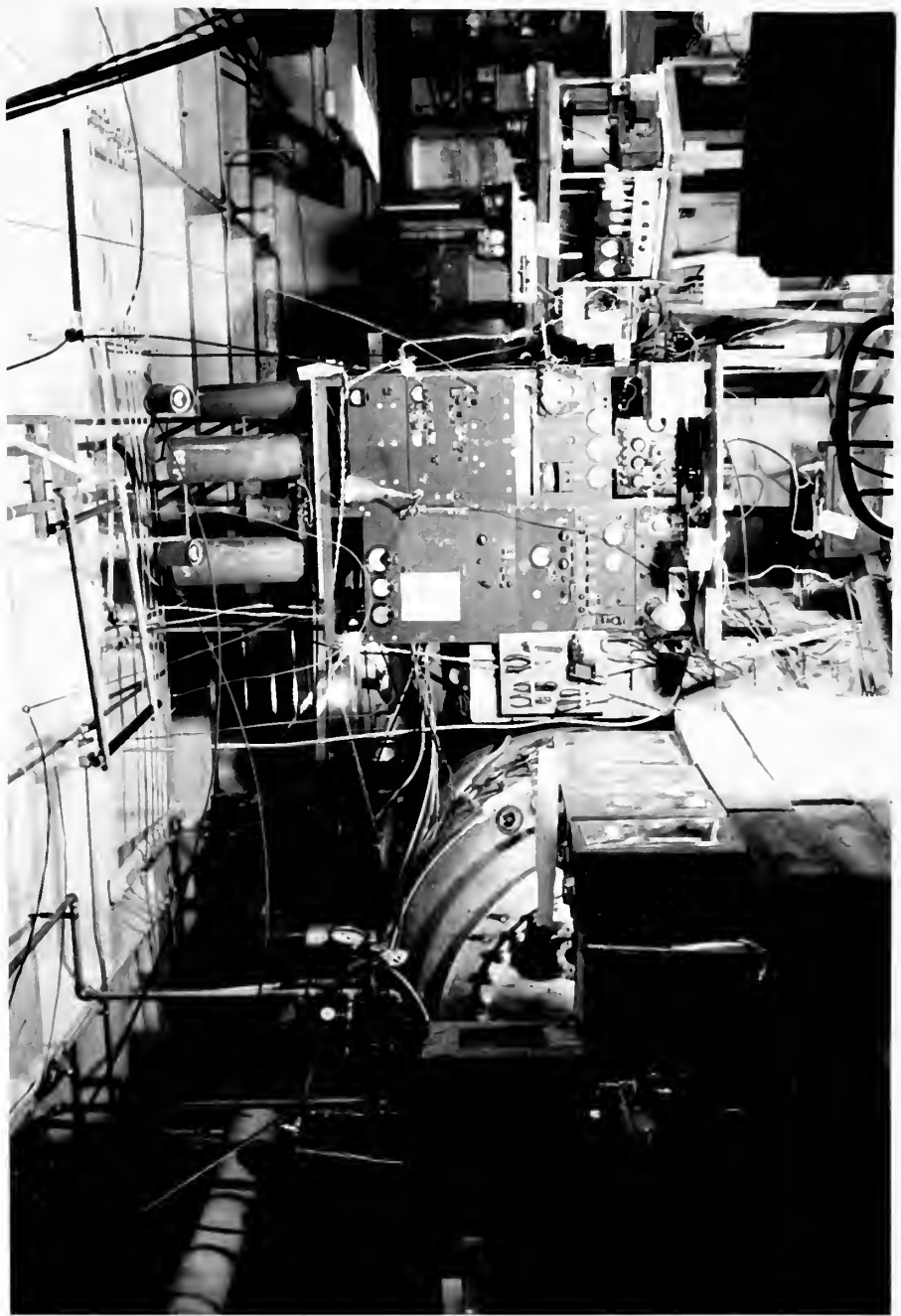
FIGURE 14

Cross section for penetration to the  
nuclear surface for two deuterons as a  
function of bombarding deuteron energy.

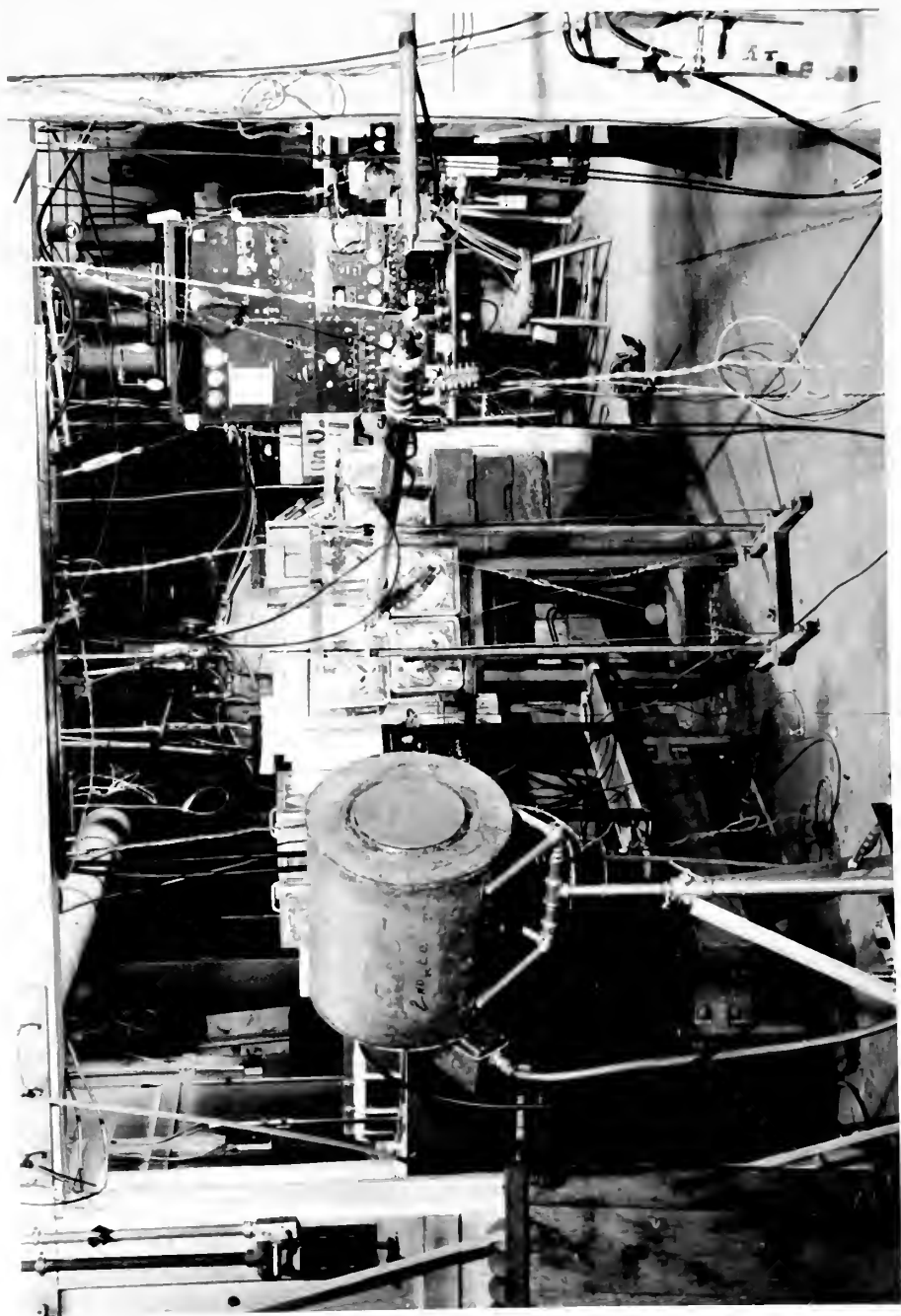


View of the high voltage generator and its control position. Automatic controlling circuits are to the right of the operators chair, shielding around the generator and the magnetic beam analyzer are shown on the left.

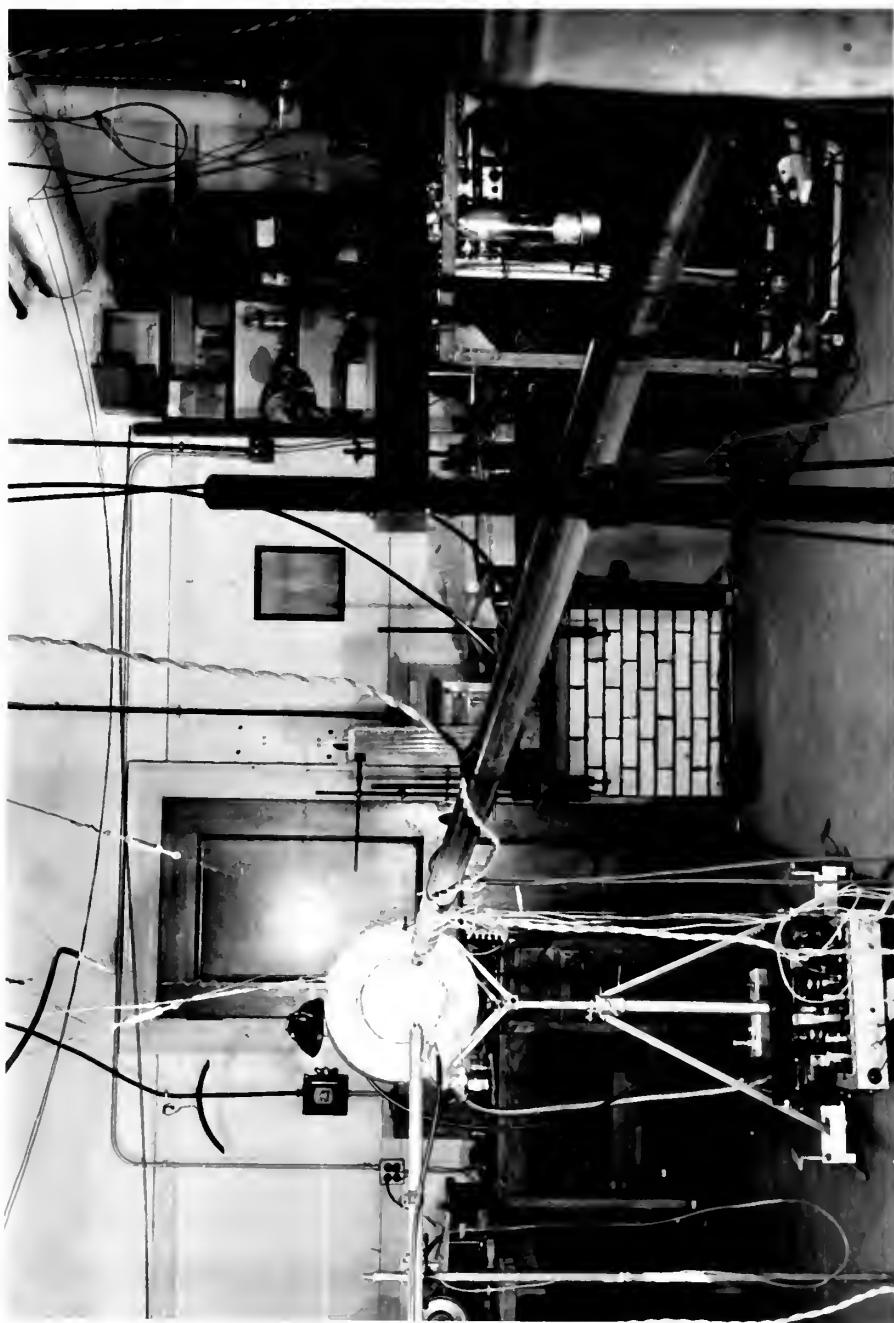




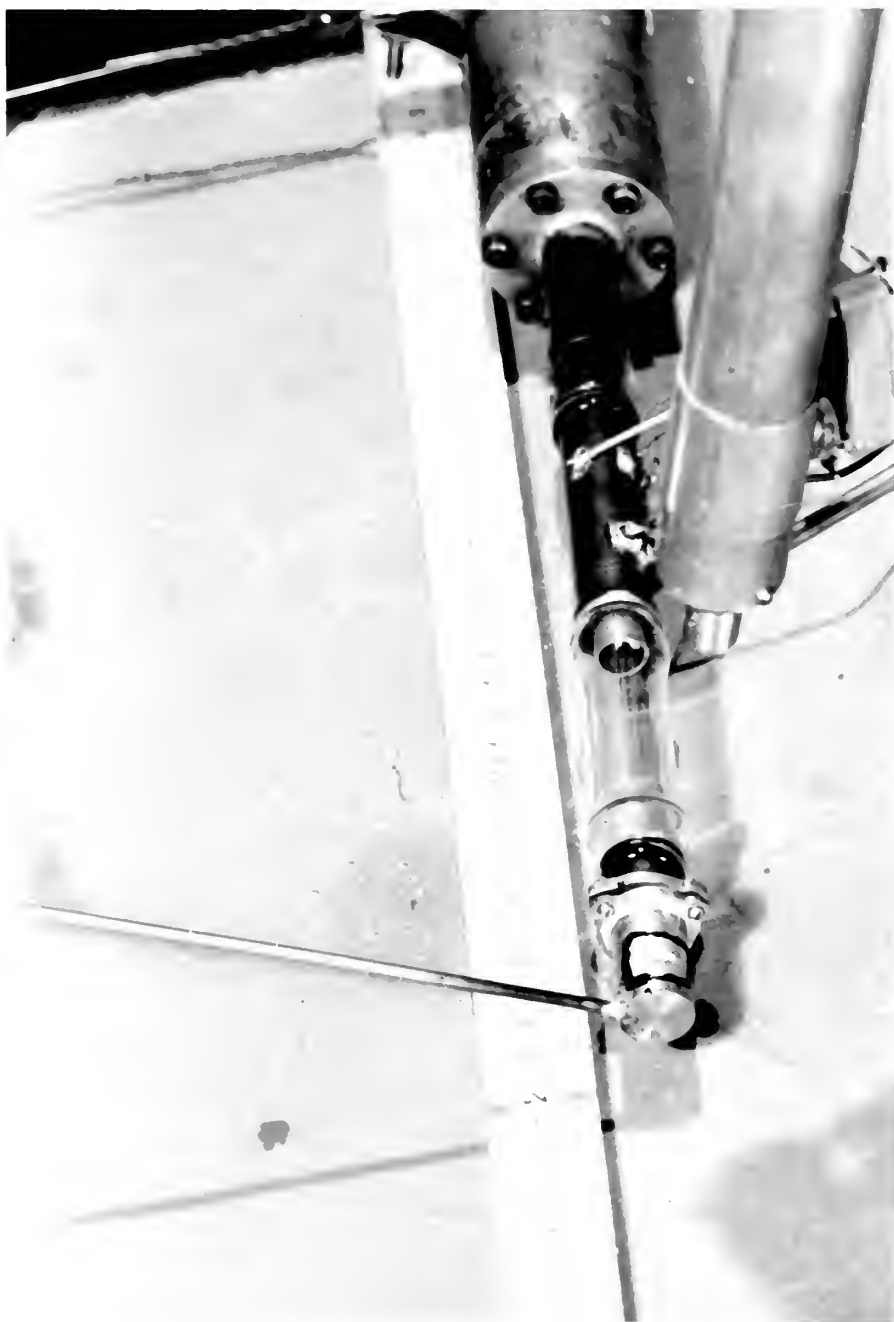
View of experimental apparatus. Gas target is in the foreground, the high voltage generator is in the background. The neutron detector is on the left of the target, the proton monitor detector is to the right of the target. Water, paraffin, and cement shielding are shown around the end of the generator and the magnetic beam analyzer.



View of experimental apparatus looking toward the target from the generator. The neutron and proton detectors are in place. Bombarding deuterons reach the target through the evacuated tube in the foreground.

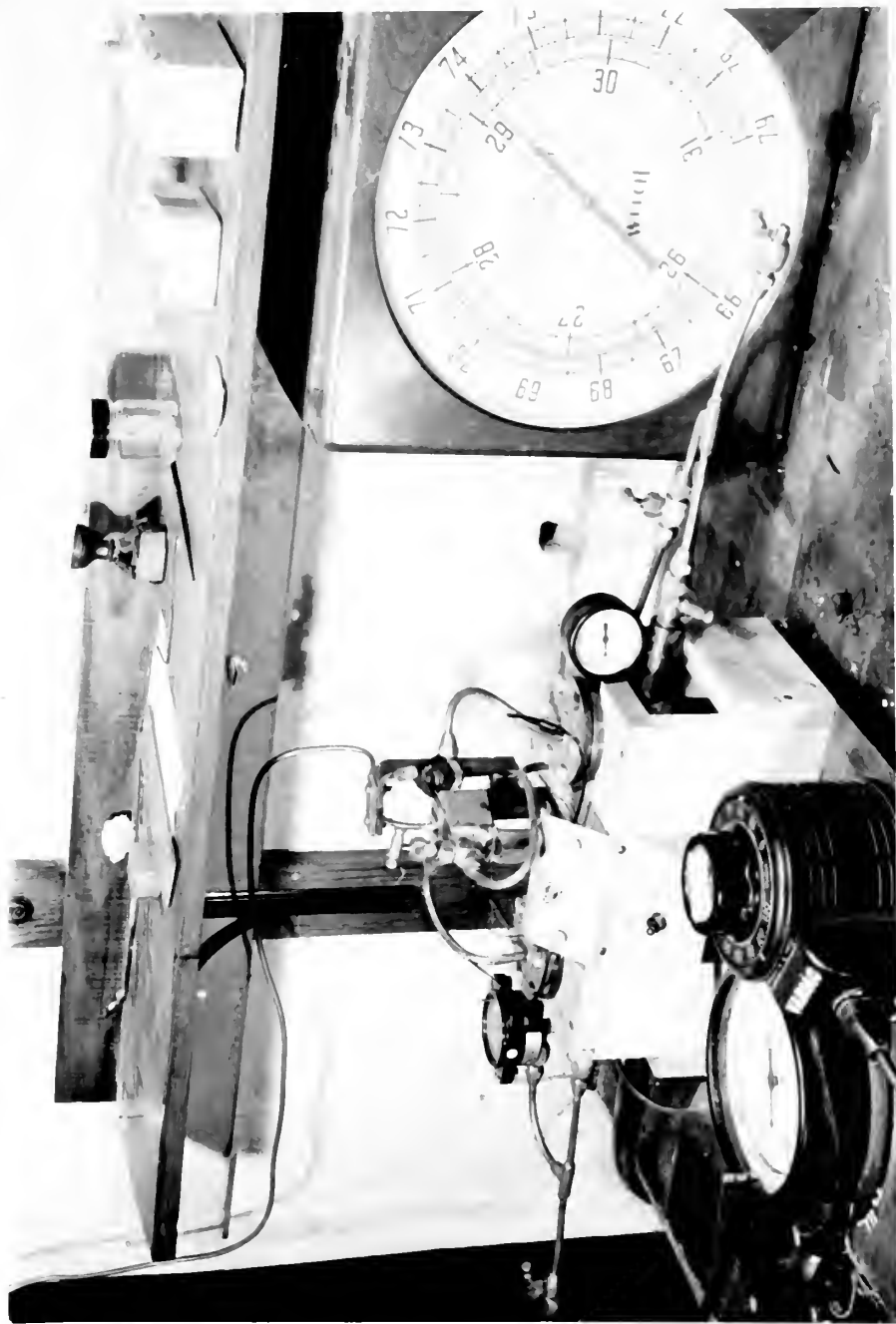


Close up view of target assembly. Gas enters target through vertical tube. Proton detector is at end of support tube at right of target.

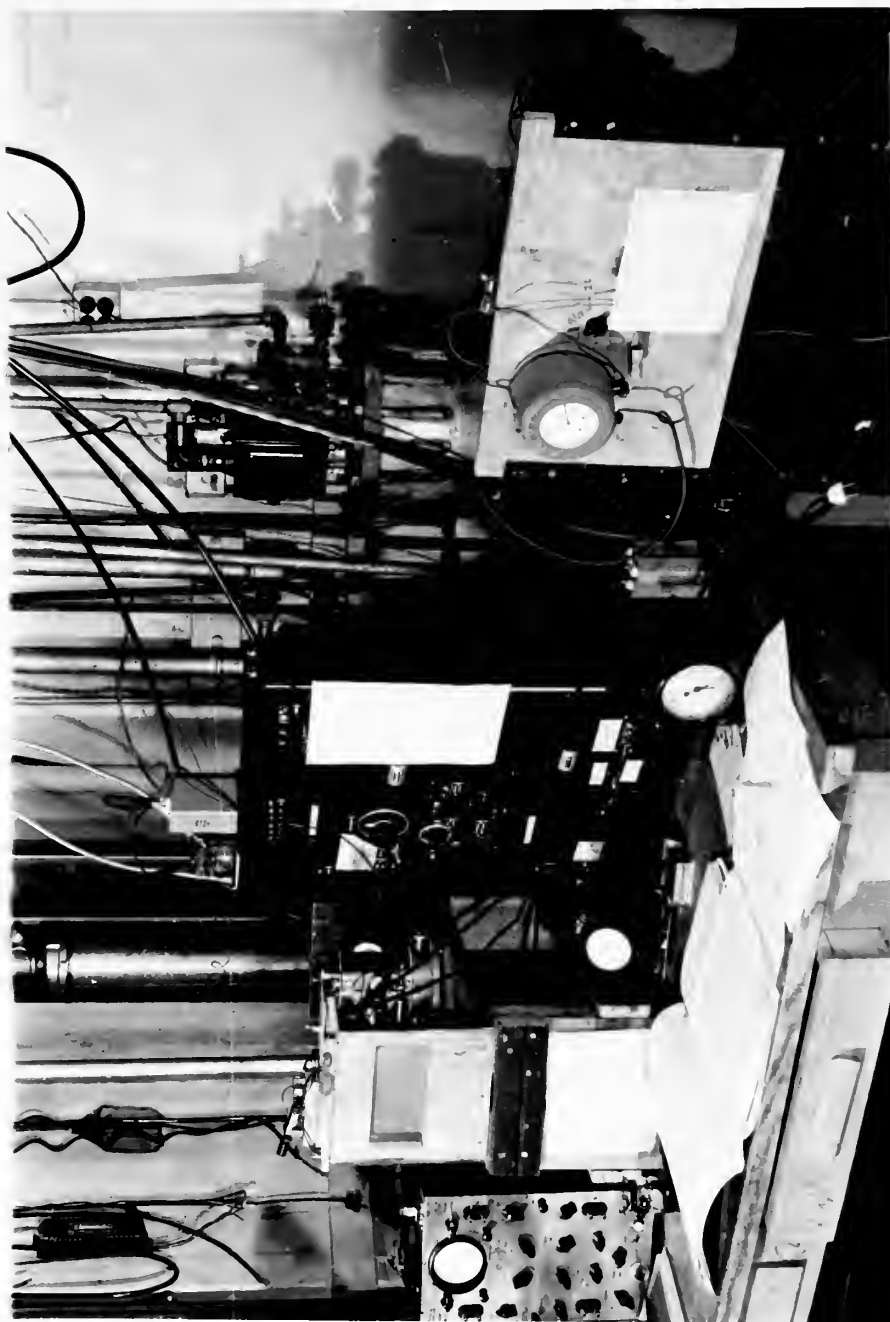


View of the gas distribution control center. Barometer and gauges for measuring gas pressures are shown. Variac is for controlling palladium leak temperature which controls rate of gas flow into target. Hydrogen and deuterium are stored in cylinders beneath valve block.





View of data recording station. Scalers, counters, recorders, timer, oscilloscope, and electrometer are shown on table. Automatic cut-off circuit is shown on the right. Generator dryer is in background.







**STOCK No. 53-C-14999**

thesH95

Excitation function and angular distribu



3 2768 002 13277 1

DUDLEY KNOX LIBRARY